Processing and Analysis of Commercial Satellite Image Data of the Nuclear Accident Near Chernobyl, U.S.S.R.

U.S. GEOLOGICAL SURVEY BULLETIN 1785

Cover: Color-composite image of Thematic Mapper spectral bands 7,4,2 with the spatial enhancement of the SPOT high-resolution visible panchromatic band. The respective dates of the data are April 29 and May 1, 1986 (SPOT Data copyright 1986 CNES).

Processing and Analysis of Commercial Satellite Image Data of the Nuclear Accident Near Chernobyl, U.S.S.R.

By FRANK G. SADOWSKI and STEVEN J. COVINGTON

U.S. GEOLOGICAL SURVEY BULLETIN 1785

DEPARTMENT OF THE INTERIOR
DONALD PAUL HODEL, Secretary

U.S. GEOLOGICAL SURVEY
Dallas L. Peck, Director

UNITED STATES GOVERNMENT PRINTING OFFICE: 1987

For sale by the Superintendent of Documents,
U.S. Government Printing Office,
Washington, DC 20402

Library of Congress Cataloging in Publication Data
Sadowski, Frank G.
Processing and analysis of commercial satellite image data of the nuclear accident near Chernobyl, U.S.S.R.
(U.S. Geological Survey bulletin ; 1785)
Bibliography: p.
Supt. of Docs. no.: I 19.3:1785
1. Chernobyl Nuclear Accident, Chernobyl, Ukraine, 1986. 2. Remote sensing—Ukraine—Chernobyl. I. Covington, Steven J. II. Title. III. Series.
QE75.B9 no. 1785 557.3 s 87-600039
[TK1362.S65] [363.1'79]

CONTENTS

FIGURES

TABLE

Processing and Analysis of Commercial Satellite Image Data of the Nuclear Accident near Chernobyl, U.S.S.R.

By Frank G. Sadowski[1] *and* Steven J. Covington[1]

Abstract

Advanced digital processing techniques were applied to Landsat-5 Thematic Mapper (TM) data and SPOT high-resolution visible (HRV) panchromatic data to maximize the utility of images of a nuclear powerplant emergency at Chernobyl in the Soviet Ukraine. The images demonstrate the unique interpretive capabilities provided by the numerous spectral bands of the Thematic Mapper and the high spatial resolution of the SPOT HRV sensor.

INTRODUCTION

This report presents the results of the processing and analysis of commercial satellite image data acquired over the nuclear powerplant at Chernobyl in the Soviet Ukraine. The images were acquired by the Landsat Thematic Mapper (TM) and the Système Probatoire d'Observation de la Terre (SPOT) high-resolution visible (HRV) sensors. Landsat is the United States' civil land remote sensing satellite system, and the SPOT satellite is operated by the French space agency Centre National d'Etudes Spatiales (CNES).

The image data were obtained in a digital format and were processed by using advanced computerized techniques that included spatial filtering, contrast enhancement, color compositing, film recording, and, in one case, data merging and color transformation. Each technique was selected and used in a manner to maximize the interpretability of the satellite images. The results of the data processing and analysis illustrate the spectral and spatial capabilities of the two sensor systems and provide information about the severity and duration of the events unfolding at the powerplant site.

Acknowledgments

The images in this report were originally produced in a very short period of time in order to be responsive to information needs that were paramount soon after the accident at the Chernobyl nuclear powerplant. The extraordinary efforts of several individuals at the U.S. Geological Survey's EROS Data Center contributed to the timely production of the image products. In particular, John L. Dwyer and Wayne A. Miller assisted in processing the Thematic Mapper data. Joy J. Hood, David J. Meyer, and June M. Thormodsgard were instrumental in processing the SPOT data and implementing the restoration and IHS software on Thematic Mapper data. Douglas R. Binnie, Ron R. Risty, Wayne A. Miller, Carolyn K. Morse, V. Annette McClaren, Susan M. Battista, and William D. Winn all had key roles in the production of final image products.

BACKGROUND

Chernobyl Nuclear Powerplant

The Chernobyl nuclear powerplant is located in the Soviet Ukraine between the towns of Chernobyl (population 25,000) and Pripyat (population 10,000). The Pripyat River, flowing past the powerplant, is one of several tributaries feeding a reservoir, which supplies freshwater to the city of Kiev located 121 km (75 mi) south of of Chernobyl (inset, fig. 1).

The powerplant is located adjacent to a pond (cooling reservoir, fig. 1), 12 km (7.4 mi) long, that supplies water to cool the reactors. The plant contains four reactors located in two separate buildings. Each reactor is capable of producing 1,000 megawatts of electrical power, making the Chernobyl plant a major source of energy for the central and western Ukraine, including the city of Kiev with its population of 2.4 million people.

As stated by the news media, the reactor that failed at Chernobyl was reactor number 4, the newest reactor at that facility, brought on line in 1983. The reactor, like the remaining three at that site, has no containment structure around it. Containment buildings are designed to prevent radiation from escaping into the atmosphere should a problem develop in the reactor core. From all accounts, an explosion occurred in the reactor core on Saturday, April 26, destroying part of the reactor building and igniting the graphite in the core. With no containment

[1]TGS Technology, Inc. Work performed under U.S. Geological Survey contract 14-08-0001-22521.

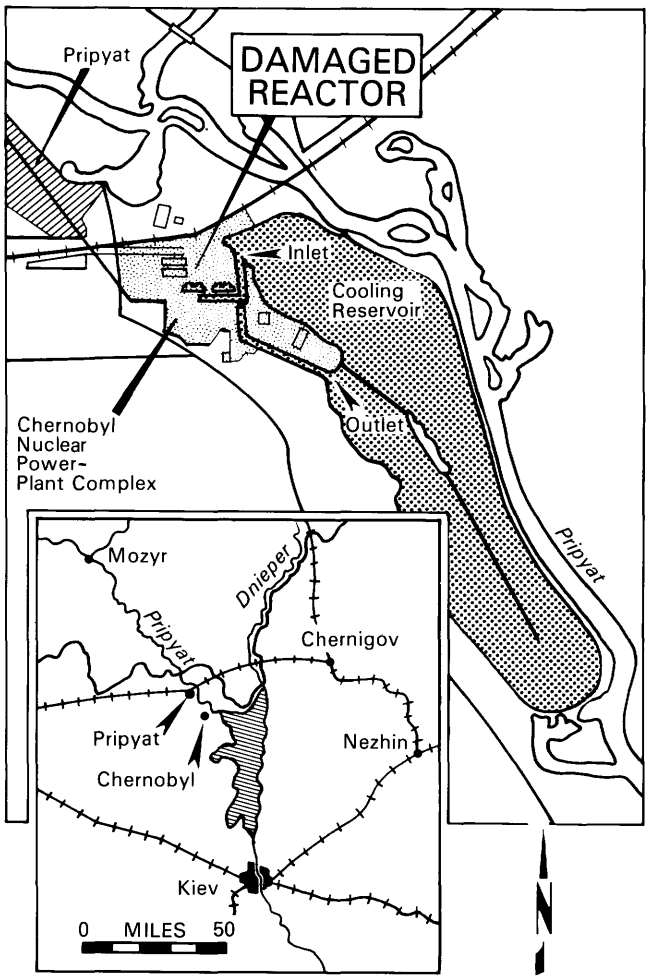

Figure 1. The location and layout of the Chernobyl nuclear powerplant (adapted from Newsweek magazine, May 12, 1986, p. 25; original artist, Christoph Blumrich).

structure, the graphite fire was exposed to the open air, allowing it to burn at intense temperatures until smothered by air-dropped mixtures of sand and boron.

Commercial Satellite Image Data

The satellite images presented in this report illustrate the current routinely available types of commercial satellite image data. The Landsat-5 TM data were acquired from the Earth Observation Satellite (EOSAT) Company of Lanham, Md., and the SPOT data were acquired from the SPOT Image Corporation, the U.S. subsidiary of the French company SPOT IMAGE. All data were purchased in computer-compatible tape format and processed at the U.S. Geological Survey's EROS Data Center in Sioux Falls, S. Dak.

The characteristics of the data and the orbiting satellites are summarized in table 1 (U.S. Geological Survey and National Oceanic and Atmospheric Administration, 1984; Courtois and Weill, 1985). The Landsat TM data and SPOT data differ markedly in their spatial and spectral characteristics. Whereas SPOT data are acquired with a smaller instantaneous field-of-view (IFOV), which contributes to finer spatial resolution, TM data have more spectral bands. Figure 2 compares the placement of the spectral bands for each sensor.

DATA ACQUISITION AND PROCESSING PROCEDURES

The images in this report include four daytime scenes of Landsat-5 TM data and one scene of SPOT HRV 10-m panchromatic data. The TM and SPOT scenes consisted of P-data and level 1B data respectively—data that have been resampled in the process of applying systematic geometric corrections. The TM and SPOT scene acquisitions are summarized as follows:

Landsat-5 TM scenes:

Date	*Path/Row*	*Quadrant*	*Landsat Scene ID*
6/06/85	181/24	3	Y5046208185X0
4/22/86	181/24	3	Y5078208140X0
4/29/86	182/24	4	Y5078908200X0
5/08/86	181/24	3	Y5079808133X0

SPOT scene:

Date	*Instrument*	*Mode*	*Scene ID*
5/01/86	HRV1	Panchromatic	S1H1860501090706

To produce images from the digital data, we used several computerized techniques of digital magnification, spatial filtering, contrast enhancement, color compositing, and film recording. Digital magnification was performed on some of the images by replicating pixel values to achieve a larger image scale. About half of the images were magnified by a spatial filtering technique designed to improve image sharpness in the TM data. The spatial filter is part of a TM image restoration software capability at the EROS Data Center (Wood and others, 1986).

Overall image contrast was enhanced by applying a piecewise linear contrast stretch to the digital data of each scene. The contrast stretch redistributes the digital data brightness values to enhance their visual analog representation on film. Due to variations in data distribution among the bands, it was necessary to create unique stretches for bands 2-7. Band 1 was not used in any image, to reduce the influence of radiometric aberrations associated with atmospheric haze. The stretches applied to the April 29, 1986, scene are presented in the Appendix.

Additional digital processing was used to merge TM and SPOT data to produce a single image in which selected spectral characteristics of the TM data and the spatial detail of SPOT 10-m panchromatic data were portrayed. The procedure included using the image restoration software to resample the 30-m TM pixels to 10-m pixels. The 10-m SPOT data were registered to the resampled TM data by using a second-order polynomial

Table 1. Characteristics of the Landsat Thematic Mapper (TM) and SPOT high-resolution visible (HRV) sensors
[M, multispectral mode; P, panchromatic mode; IFOV, instantaneous field of view. --, not applicable]

	Landsat-5 TM	SPOT HRV
Launch date	March 1, 1984	February 21,1986
Spectral bands (in micrometers)		
1	0.45-0.52	0.50-0.59 (M), 0.51-0.73 (P)
2	0.52-0.60	0.61-0.68 (M)
3	0.63-0.69	0.79-0.89 (M)
4	0.76-0.90	--
5	1.55-1.75	--
6	10.40-12.50	--
7	2.08-2.35	--
Ground IFOV	30 m × 30 m (Bands 1-5, 7) 120 m × 120 m (Band 6)	20 m × 20 m (M)* 10 m × 10 m (P)*
Orbit inclination (degrees)	98.2	98.7
Orbital altitude (kilometers)	705	832
Orbital nodal period (minutes)	98.9	101.4
Orbits per day	14.6	14.2
Equatorial crossing time (local solar time)		
Descending	9:39 a.m.	10:30 a.m.
Ascending	9:39 p.m.	--
Repeat period (days)	16	26
Ground swath (kilometers)	185	117 when the two HRV instruments are pointed so as to cover adjacent fields, with 3 km overlap at nadir. 60 at nadir. 80 at extreme off-nadir.**

* At nadir.
** Sensor design allows ±27 degrees off-nadir viewing capabilities.

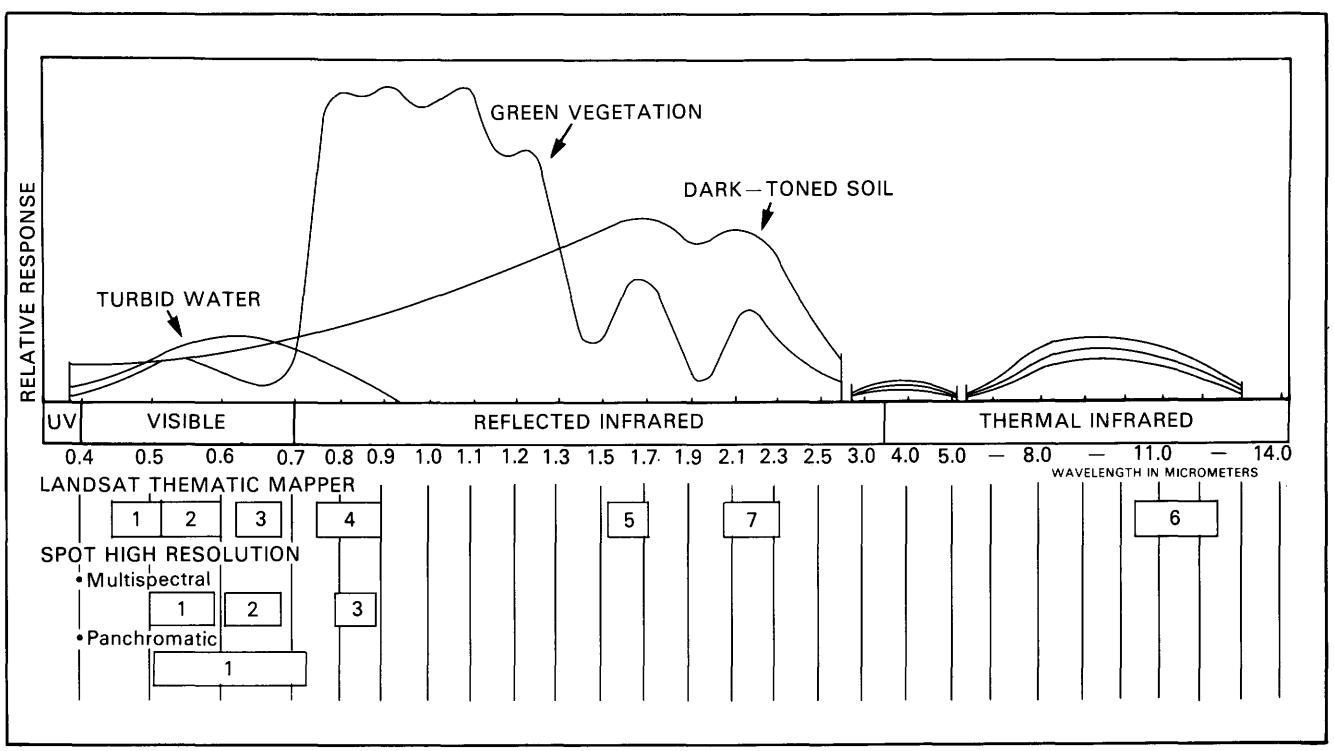

Figure 2. Spectral band placement for the Landsat Thematic Mapper and the SPOT high-resolution visible sensors.

spatial model derived from 18 control points. The two data sets were then merged by using an intensity, hue, and saturation (IHS) transformation (Haydn and others, 1982). This transformation maintained the hue (color) relationships of a selected three-band combination of TM data, while modulating the intensity of the TM data with values derived from the higher resolution SPOT data. Finally, the merged IHS data were transformed back into red-green-blue color space for reproduction on photographic film.

Prior to creation of a film product of each image, annotation and collar work were digitally inserted into the scenes for informational content and reference. Color images were recorded onto Kodak[2] 2445 Aerocolor negative film using a Color FIRE 240 film recorder. The Color FIRE film recorder creates a color image by assigning an additive primary color (red, green, or blue, abbreviated R,G,B) to each of three selected spectral bands of the digital data. As an example, a combination of TM spectral bands 7,4,2 in R,G,B sequence would have band 7 assigned to the red Color FIRE channel, band 4 to the green channel, and band 2 to the blue channel.

IMAGE PRODUCTS AND INTERPRETATIONS

The image data acquired in each of the TM spectral bands on April 29, 1986, for the immediate area of the reactor site are presented in figure 3. In most circumstances, the levels of brightness associated with ground features in TM bands 1 through 5 and band 7 are attributable to solar reflectance. Figure 3 illustrates the relative changes in reflectance that occur for various ground features from band to band. Brightness variations in band 6 are attributable to emitted energy received at the sensor in the thermal infrared wavelength region; generally, warmer objects are brighter. The somewhat blurred appearance of the band 6 image is due to the coarser (120-m) IFOV that results in lower spatial resolution (table 1).

When the multispectral data represented in figure 3 are interpreted in conjunction with knowledge of terrain reflectance and emittance phenomena, a number of technical observations can be made about the conditions at the reactor site on April 29, following the disaster reported to have occurred on April 26. These observations are enhanced by comparing the image data of April 29 to additional TM images of the site acquired before (June 6, 1985, and April 22, 1986) and some 12 days after (May 8, 1986) the disaster.

Figures 4 and 5 show a regional view of the Chernobyl site on April 29. These images readily lend themselves to evaluations of agricultural, forest, and wetlands areas in the region. Figure 4 includes spectral bands 4,3,2 combined in the R,G,B color sequence. This combination provides the traditional color-infrared image, widely used for interpreting vegetation and soils information. Inspection of this color-composite image at larger scale provides some evidence of a darkened strip of ground on the west side of the reactor building that is not evident on earlier dates. However, additional information about the condition of the reactor is not apparent.

Figure 5 includes TM band 7—a longer wavelength near-infrared spectral band—in combination with TM bands 4 and 2 (R,G,B sequence). A large-scale view of the reactor site in this same band combination is shown in figure 6. A bright red spot can be seen in the powerplant complex near the location of reactor number 4, the farthest one from the cooling pond (see sketch in fig. 1). The color of the spot indicates a high brightness value in band 7 and corresponding low values in bands 4 and 2. This somewhat unusual combination of brightness values is indicative of a very high temperature heat source, suggesting the exposed burning graphite of the damaged reactor.

Consideration of radiation theory and the analysis of brightness values in TM bands 1 through 5 and TM band 7 of the April 29 TM image provide evidence to support the interpretation of the red spot as a high-temperature heat source. In figure 7, the TM spectral bands have been superimposed on a set of radiant emission curves for selected objects at different temperatures. The curves demonstrate that terrain features near ambient temperatures of 290 K (17°C) radiate energy at long-wavelength regions, with a peak between 10 and 12 μm (vicinity of TM band 6). However, as a feature becomes hotter, the intensity of the emitted energy increases and the radiation peak shifts toward shorter wavelengths. If the emitting feature's temperature was about 1,000 K (727°C), one would expect the emission peak to occur near the region of TM band 7 and, to lesser degrees, in TM band 5 and the progressively shorter wavelength spectral bands.

An analysis of the brightness values in the April 29 TM image provides results that are consistent with the above expectation. Figure 8 shows brightness values over the location of the damaged reactor compared with brightness values for portions of the adjacent undamaged reactor structure. The brightness values for the undamaged structure are relatively low in all bands, suggestive of reflectance from a dark (perhaps asphalt) roof surface. Brightness values over the damaged reactor, while equivalent to those of the undamaged reactor structure in TM bands 1 through 4, display the increase in TM band 5 and, most noticeably, in band 7 that is

[2]Any use of trade names and trademarks in this publication is for descriptive purposes only and does not constitute endorsement by the U.S. Geological Survey.

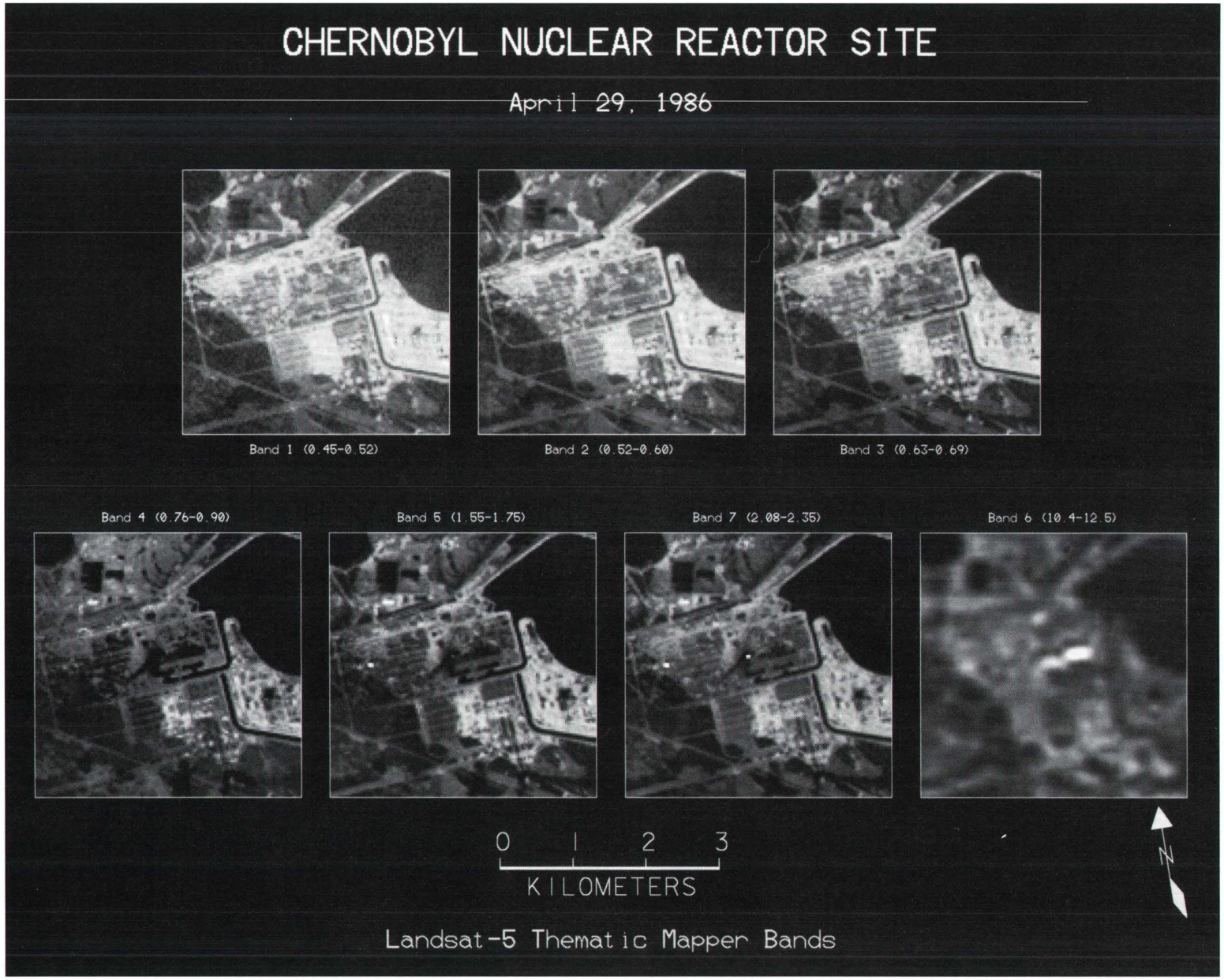

Figure 3. Image data acquired in each of the Thematic Mapper spectral bands on April 29, 1986.

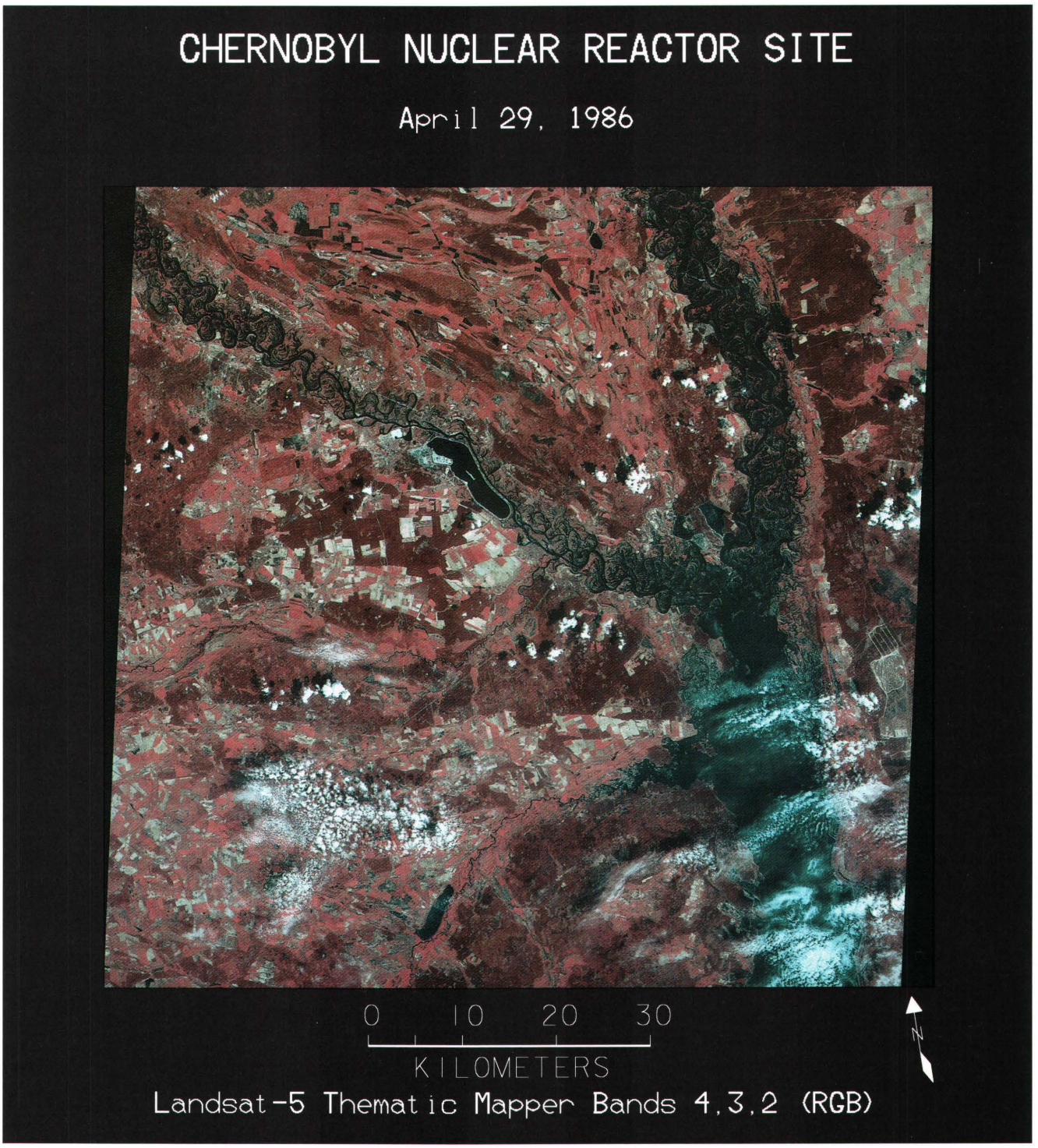

Figure 4. Color-composite image of a Thematic Mapper quarter-scene showing a regional view of the Chernobyl site on April 29, 1986. The spectral band combination is bands 4,3,2 (red,green,blue sequence).

Figure 5. Color-composite image of a Thematic Mapper quarter-scene showing a regional view of the Chernobyl site on April 29, 1986. The spectral band combination is bands 7,4,2 (red,green,blue sequence).

Figure 6. Color-composite image of Thematic Mapper spectral bands 7,4,2 (red,green,blue sequence) acquired on April 29, 1986.

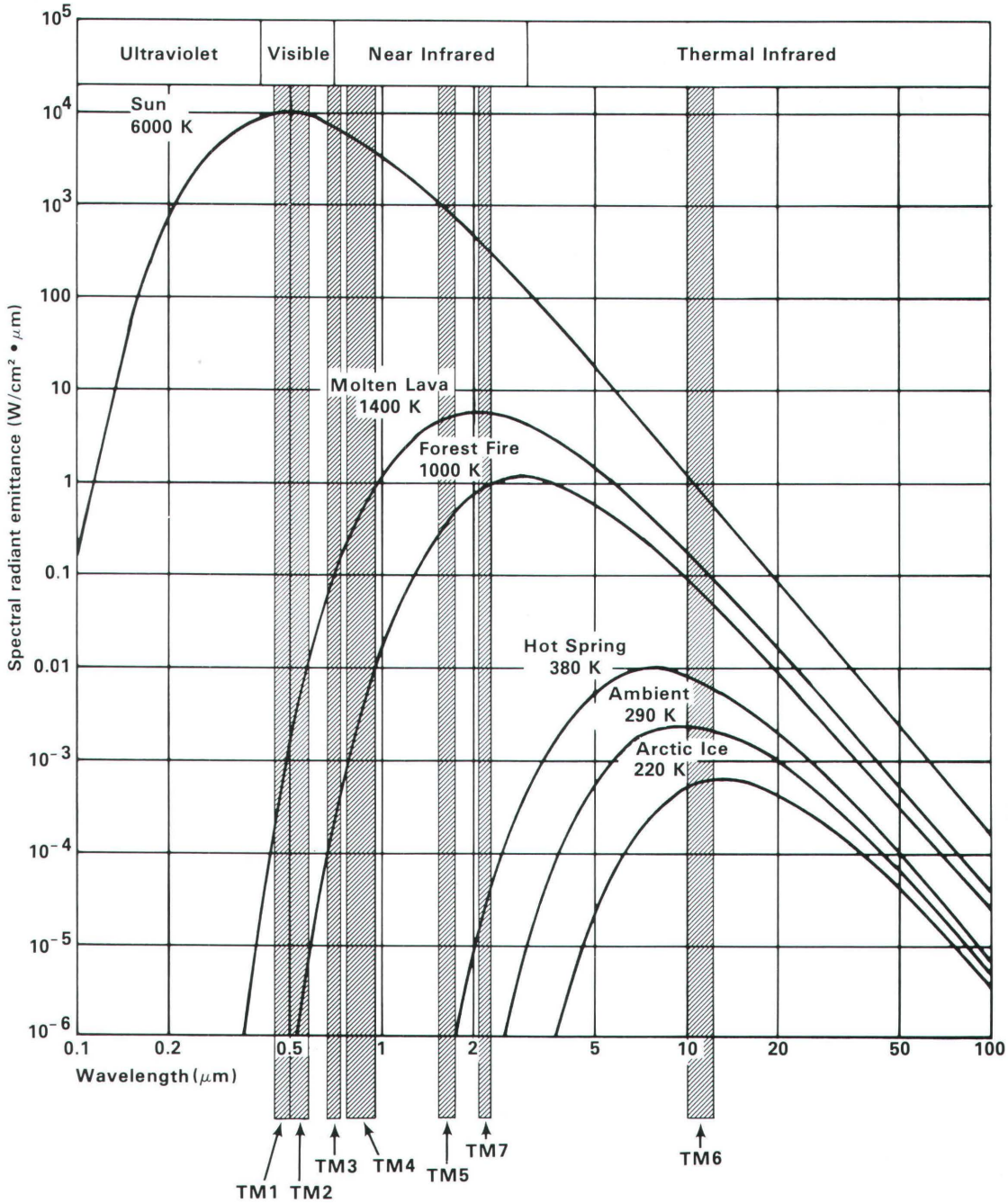

Figure 7. Thematic Mapper spectral bands superimposed on the radiant emission spectra of selected objects.

characteristic of a very hot heat source. The differences in brightness values between the damaged reactor and the adjacent undamaged structure in each of bands 5 and 7 can be attributed to the emitted component of total radiation observed by the sensor.

The unambiguous interpretation of the damaged reactor requires knowing the brightness values of ground features in other bands in addition to TM band 7. The brightness values of the sand bar (from the river adjacent to the reactor complex) in figure 8 show that while some ground features can have equivalent brightness in TM band 7, their brightness in other TM bands helps to identify them as natural or man-made features having generally high solar reflectance. This observation applies also to the bright spot that appears at the left edge of the powerplant complex in figure 6. Although the identity of this feature is uncertain, its brightness values in all TM bands are not consistent with those of a high-temperature

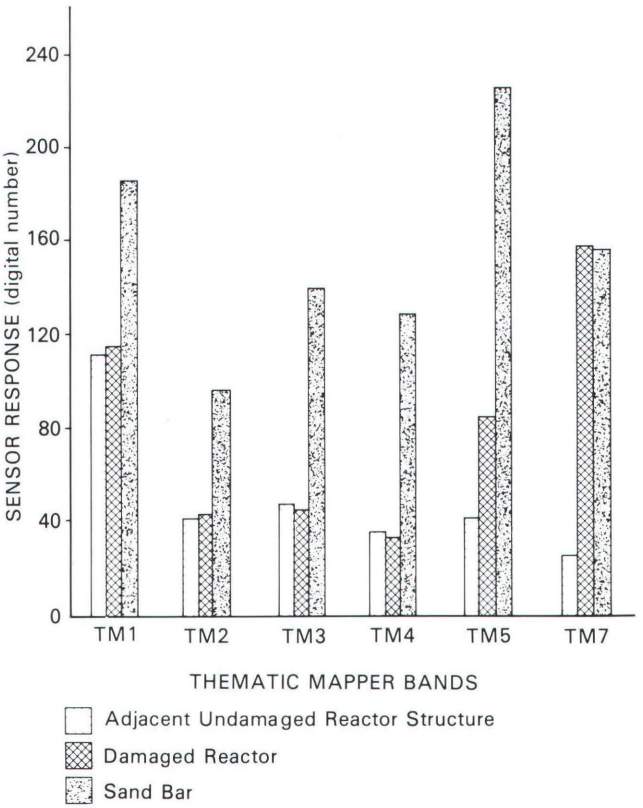

Figure 8. Brightness values of ground features in the Thematic Mapper data of April 29, 1986.

heat source. The color-composite image of bands 7,4,2 (R,G,B sequence) readily enables making such multispectral observations.

Figures 9-11 show TM images from additional dates of observation over the Chernobyl reactor site that enable us to interpret changes related to the disaster. The image of April 22, 1986 (fig. 10), shows little obvious difference from the image acquired on June 6, 1985, suggesting that just before the disaster the reactor site was functioning much as it was nearly a year earlier. The image of April 29, 1986 (fig. 6), shows the anomalous heat source from reactor number 4 and the darkened strip of ground on the west side of the reactor that may have resulted from the explosions and (or) from reported attempts to smother the exposed burning graphite with helicopter-borne loads of sand and boron. The image of May 8, 1986 (fig. 11), shows that the bright red spot associated with the damaged reactor is no longer evident in TM band 7, indicating that the apparent temperature had dropped considerably since April 29. Also, the water intake channels immediately south of the reactor structure appear dry, suggesting that the water supply inlet from the cooling pond is closed.

Figure 12 enables comparison of the relative temperature of ground features in TM band 6 on each of the four dates. The high-temperature heat source associated with the damaged reactor does not appear on the April 29 image because TM band 6 is designed to be sensitive to the temperature range of 200 K to 340 K (-70°C to 70°C). This means that the very high apparent temperature of the damaged reactor cannot be detected. Under ideal conditions, the damaged reactor can only be detected as a feature at 340 K, only slightly higher than the ambient temperature of most terrain features. Given this lack of thermal contrast, the coarse 120-m IFOV of TM band 6 inhibits detection of the localized heat source. However, the brightness values of large, moderately warm structures in the reactor complex such as the turbine/generator halls are readily obvious on each date. It can be seen that the apparent temperature of these structures does not change dramatically between dates, even after the disaster, thus offering little indication of the disaster occurrence.

The images in figure 12 show the thermal patterns of water in the cooling pond on each date studied. In figure 13, these thermal patterns have been color-coded relative to the adjacent river for the three dates that occur just before, during, and after the crisis associated with the burning reactor. The image of April 22 illustrates the temperature gradient of the cooling pond during normal operation. Warm (red) water, discharged from the plant at the outlet channel, is cooled as it circulates around the pond in a counterclockwise direction and then reenters the plant at the inlet channel. This temperature gradient is not evident on April 29 or May 8, clearly indicating that the entire pond has approached a near-uniform temperature due to the cessation of normal operations on April 26. The overall pond temperature was still warmer than the river on April 29, and it had cooled to very near the river temperature by May 8. (The land area in these images is represented by the reflectance patterns in TM band 4; thus, land brightness values have no relationship to relative temperature.)

Figure 14 shows the Chernobyl reactor site as acquired by the high-resolution visible (HRV) imaging sensor of the French SPOT satellite on May 1, 1986. The 10-m spatial resolution of this panchromatic image reveals greater spatial detail in the vicinity of the reactor site than noted on the TM images.

The result of combining the 10-m spatial resolution of the SPOT data with the multispectral (bands 7,4,2) data of the Thematic Mapper is shown in figure 15. This image vividly illustrates the advantages of each of these two types of commercial satellite image data. Simply stated, much of the multispectral information available only in the TM data can be observed in the context of the higher spatial resolution SPOT data.

Figure 9. Color-composite image of Thematic Mapper spectral bands 7,4,2 (red,green,blue sequence) acquired on June 6, 1985.

Figure 10. Color-composite image of Thematic Mapper spectral bands 7,4,2 (red,green,blue sequence) acquired on April 22, 1986.

Figure 11. Color-composite image of Thematic Mapper spectral bands 7,4,2 (red,green,blue sequence) acquired on May 8, 1986.

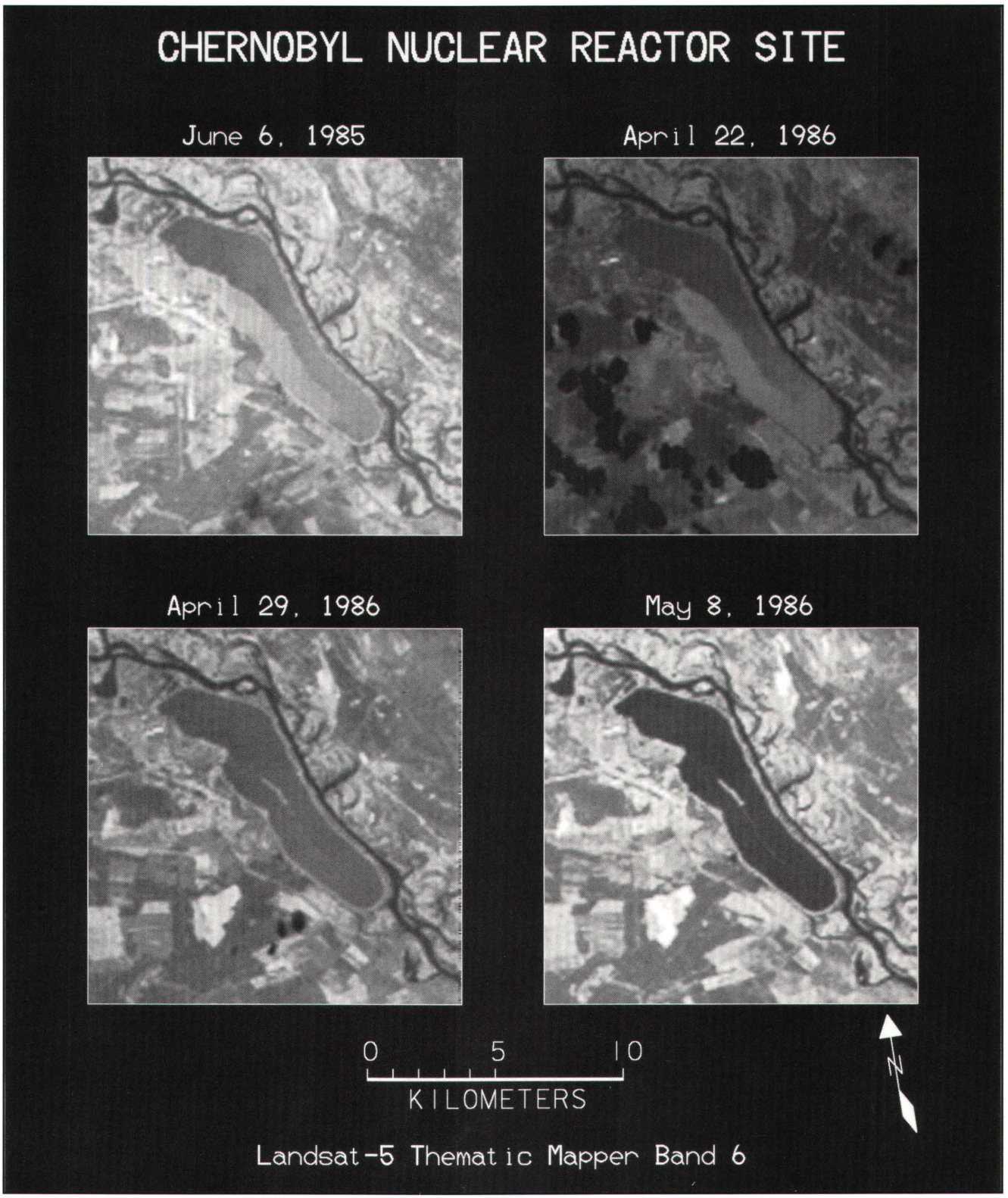

Figure 12. Images of Thematic Mapper band 6 (thermal band) for the four dates studied.

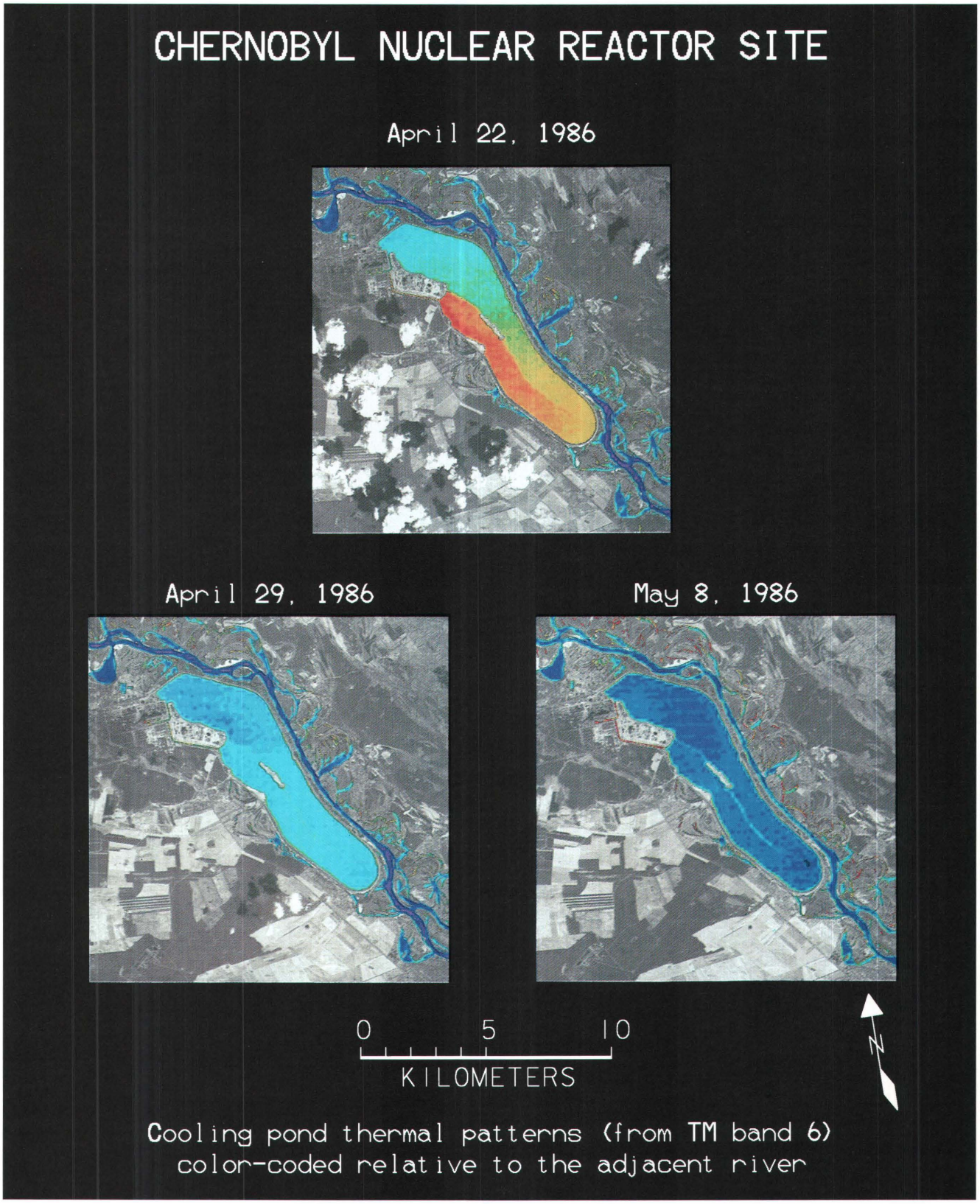

Figure 13. Images showing cooling pond thermal patterns from TM band 6, color-coded relative to the adjacent river, for each of three dates. (Land brightness values are from TM band 4.)

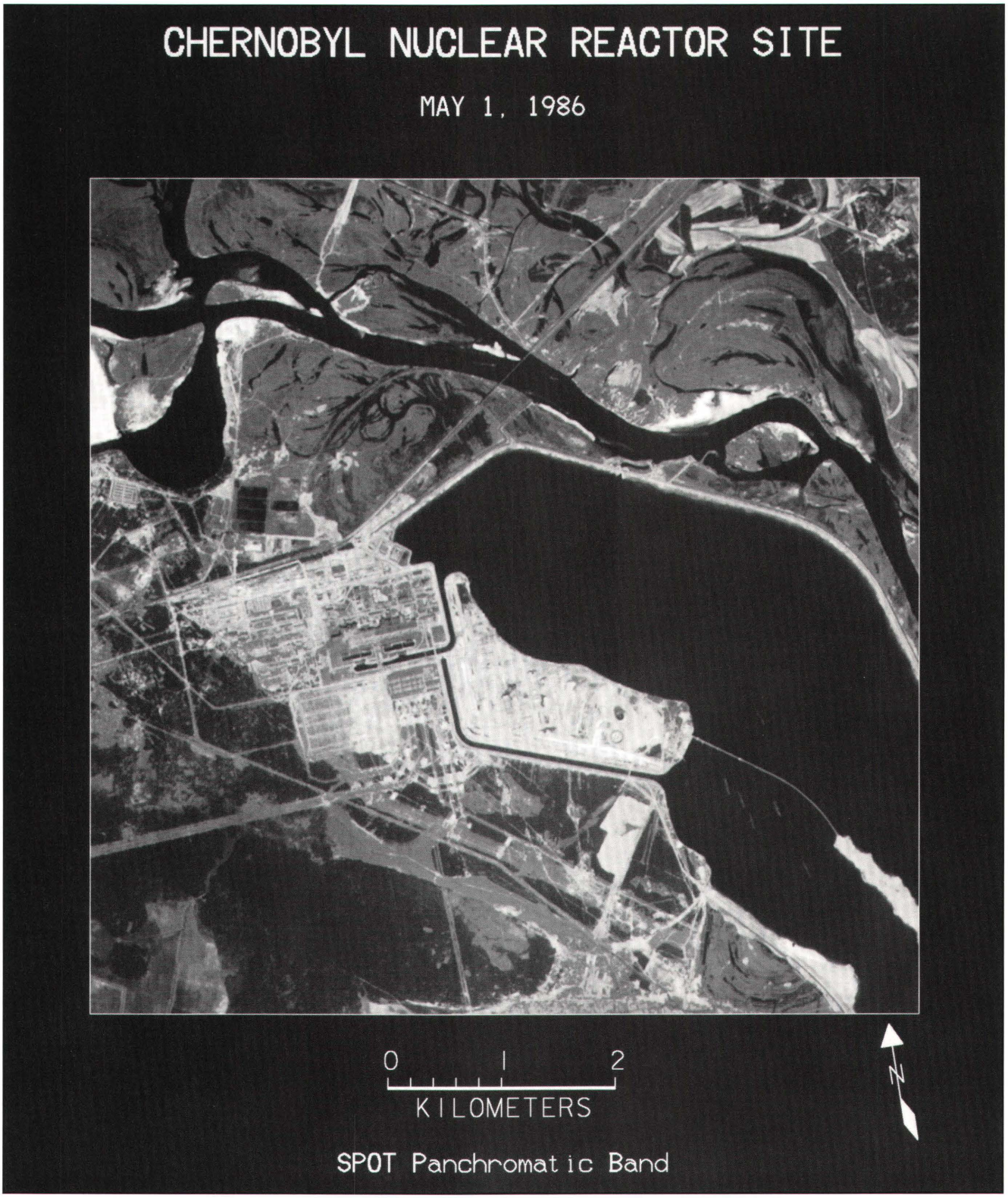

Figure 14. SPOT high-resolution visible panchromatic image acquired on May 1, 1986 (SPOT Data © 1986 CNES).

Figure 15. Color-composite image of Thematic Mapper spectral bands 7,4,2 with the spatial enhancement of the SPOT high-resolution visible panchromatic band. The respective dates of the data are April 29 and May 1, 1986 (SPOT Data © 1986 CNES).

CONCLUSIONS

Images of Landsat-5 TM data and SPOT HRV panchromatic data acquired over the Chernobyl nuclear powerplant have illustrated the following spectral and spatial capabilities and limitations of currently available commercial satellite image data:

- The Landsat Thematic Mapper can show direct evidence of high-temperature heat sources in the long-wavelength near-infrared spectral bands unique to this sensor. TM data of April 29, 1986, showed intermediate and high brightness values for the damaged reactor in TM bands 5 and 7, respectively, that are attributed to emitted (thermal) radiation from the exposed burning graphite. A color-composite image of bands 7,4,2 (R,G,B sequence) was particularly useful for observing the damaged reactor.
- TM band 6 (the thermal band) showed no high-temperature response from the damaged reactor due to the limited range of temperature response designed for this band and the coarse 120-m IFOV. This band was specifically designed to be highly sensitive to temperature variations in earth surface features that are near ambient air temperature. As an example, TM band 6 enabled us to observe differences in water-temperature gradients in the cooling pond adjacent to the powerplant complex before and after the disaster.
- The SPOT 10-m panchromatic image revealed significantly greater spatial detail in the vicinity of the reactor site. Shadow details associated with larger features may allow for approximations of heights.
- An image of merged TM and SPOT data enabled us to observe much of the multispectral information available only in the TM data in the context of the higher spatial resolution SPOT data.

The response of TM bands 5 and 7 to the emitted radiation from the damaged reactor provides evidence to suggest broader application of these spectral bands for detecting and monitoring other high-temperature thermal anomalies on the earth's surface. Studies elsewhere have begun to demonstrate application to thermal features of active volcanoes. These include the use of TM band 7 for portraying the intense heat emission of a volcano in eruption (EOSAT Corporation, 1986) and a recent discovery of a significant thermal anomaly on Lascar volcano in northern Chile (P.W. Francis and D.A. Rothery, written commun., 1986). At the EROS Data Center, evaluations of band 5 and, more importantly, band 7 in TM images have provided the capability to observe the flames at the perimeter of rangeland fires in east-central Africa.

An analysis of TM images acquired before and after the disaster enabled several technical observations about the conditions of the reactor site:

- An image of April 22, 1986, showed little obvious difference from an image acquired on June 6, 1985, suggesting that, four days before the accident, the reactor site was functioning much as it was nearly a year earlier.
- An image of May 8, 1986, showed that the high brightness values associated with the damaged reactor in TM bands 5 and 7 on April 29, 1986, were no longer evident, indicating a significant reduction in the apparent temperature of the damaged reactor.
- A darkened strip of ground on the west side of reactor number 4, evident on the two images following the disaster, may be a blast effect that resulted from the explosion or debris associated with reported attempts to smother the exposed burning graphite with sand and boron.
- Water intake channels adjacent to the south side of the reactor structure appear to be dry on May 8, suggesting that the water supply inlet from the cooling pond is closed.
- Images of TM band 6 show a large gradient in water temperature in the cooling pond during the normal operation of the plant on June 6, 1985, and April 22, 1986. The lack of a water-temperature gradient in the pond on April 29 and May 8, 1986, indicates that the entire pond has approached a near-uniform temperature due to the cessation of normal operations.

REFERENCES

Courtois, M., and Weill, G., 1985, The SPOT satellite system, *in* Schnaph, A., ed., Monitoring Earth's oceans, land, and atmosphere from space—Sensors, systems, and applications; v. 97 of Progress in Astronautics and Aeronautics: New York, American Institute of Aeronautics and Astronautics, Inc., 830 p.

EOSAT Corporation, 1986, Augustine volcano Thematic Mapper image: Landsat Data Users Notes, v. 1, no. 3, p. 1-2.

Haydn, R., Dalke, G., Henkel, J., and Bare, J., 1982, Application of the IHS color transform to the processing of multisensor data and image enhancement, *in* International Symposium on Remote Sensing of Environment, First Thematic Conference: Remote Sensing of Arid and Semi-Arid Lands, Cairo, Egypt, January 1982, Proceedings: Environmental Research Institute of Michigan, Ann Arbor, Mich., p. 599-616.

U.S. Geological Survey and National Oceanic and Atmospheric Administration, 1984, Landsat 4 data users handbook: Reston, Va., U.S. Geological Survey.

Wood, L.M., Schowengerdt, R.A., and Meyer, D.J., 1986, Restoration for sampled imaging systems, *in* Applications of Digital Image Processing IX, SPIE International Symposium on Optical and Optoelectronic Applied Sciences and Engineering, 30th, Proceedings: San Diego, Calif., v. 697, p. 333-340.

Appendix. Digital values of the piecewise linear contrast stretches applied to the April 29, 1986, Thematic Mapper (TM) data

TM Band											
2		3		4		5		6		7	
Input	Output	Input	Output	Input	Output	Input	Output	Input	Output	Input	Output
0	0	0	0	0	0	0	0	0	0	0	0
28	0	27	0	15	0	7	0	105	0	39	115
41	115	46	128	37	40	34	40	132	135	100	210
66	210	83	210	55	140	75	130	156	255	160	255
92	255	121	255	104	220	137	210	255	255	255	255
255	255	255	255	172	255	200	255				
				255	255	255	255				


U.S. DEPARTMENT OF THE INTERIOR
March 3, 1849